Tikrit Journal of Engineering Sciences

IRAQI Academic Scientific Journals | TJES Tikrit Journal of Engineering Sciences

Article | Tikrit Journal of Engineering Sciences (2026); 33 (1): 2453

Open Access

Miniaturized and Low SAR Printed Antenna for Healthcare Monitoring

Abu Obaydah N. Khazaal, Mohammed K. S. Al-Mashhadani *

Electrical Engineering Department, College of Engineering, Tikrit University, Tikrit, Iraq.

Emails:

Abu Obaydah N. Khazaal | Mohammed K. S. Al-Mashhadani

Abstract:

A miniaturized medical antenna with dual-band operation in the Industrial, Scientific, and Medical (ISM) bands is presented with a low specific absorption rate (SAR) for recommended safety limits. The proposed antenna with dimensions (27.6 mm × 28.2 mm × 0.32 mm) is considered suitable for medical applications. A fractal copper patch, Rogers 3010 biocompatible material, and full ground plane copper are used to get a miniature Antenna design. The research aims to design a compact, biocompatible, and low-SAR medical antenna for implantable and wearable applications. The dual-band antenna uses a fractal copper patch, simulating performance using CST Studio Suite, and optimizing SAR and gain for safety. Different configurations are analyzed for efficiency and medical applications. Low SAR levels were achieved for implantable and wearable designs equal to (0.487, and 0.141 W/kg) and (0.488, and 0.0392 W/kg) for dual bands 0.9 and 2.4 GHz respectively, and Negative gain for safety considerations .The design has been developed into three different forms: implantable, wearable, and capsule design for higher efficiency and more medical applications. The CST studio suite's simulations assessed the antenna's performance using design standards rules and efforts.

Keywords:

Biocompatible materials; Dual-band ISM; Low SAR; Medical antenna; Miniaturized design.

Highlights:

- Design of a miniaturized biomedical antenna for dual-band ISM applications.
- Use of biocompatible materials and a compact copper patch for safe medical integration.
- Optimization of low Specific Absorption Rate (SAR) through advanced simulation techniques.

Corresponding Author*:

Mohammed K. S. Al-Mashhadani

Electrical Engineering Department, Tikrit University, Tikrit, Iraq.

Article History:

Received:	18 Dec. 2024
Received in revised form:	07 Feb. 2025
Accepted:	27 Feb. 2025
Final Proofreading:	25 Jun. 2026
Available online:	11 Aug. 2026

Citation:

Abu Obaydah N. Khazaal, Mohammed K. S. Al-Mashhadani. **Miniaturized and Low SAR Printed Antenna for Healthcare Monitoring**. *Tikrit Journal of Engineering Sciences* 2026; **33**(1): 2453.

https://doi.org/10.25130/tjes.33.1.35

1.INTRODUCTION

Biomedical antennas have attracted the attention of researchers and designers for the best practical and medical results. Biomedical antenna is essential for wireless communication with medical devices. These antennas face several issues that must be solved, like differences in dielectric characteristics within the human body, which impact antenna work, and the Specific Absorption Rate (SAR) for personal protection. Specifically, the antenna's miniaturization must be considered due to the size constraints of medical devices. So, diverse methods and techniques for an integrated size are suggested [1-4]. Several frequency bands are utilized for clinical implantable devices. To save battery life and extend the lifespan of the medical device, designers typically use the dual-band (ISM) to toggle between sleep and wake modes. Negative gain in medical antennas is a necessary factor for patient safety. It helps reduce the amount of energy absorbed by tissues, limits SAR, and reduces electromagnetic interference, making medical devices implanted or used next to the body safer [5, 6]. The ISM bands differ by area and contain certain globally known frequencies, such as [7]:

- 13.56 MHz: Used for RFID systems and near-field communication NFC.
- 27.12 MHz: Industrial heating and medical devices.
- 433 MHz: Short-range communication devices.
- 915 MHz: Common in industrial applications, and wireless sensor networks.
- 2.4 GHz: The most well-known band, used in Wi-Fi, Bluetooth, and microwave ovens.
- 5.8 GHz: Another band used in wireless networks, radar, and ISM equipment

ISM bands are the Unlicensed Frequency Bands used for instrumentation, for industrial, scientific, and medical applications. These are working at 433.05–434.79 MHz, 902–928 MHz, 2.4–2.480 GHz, and 5.725–5.875 GHz bands. They are used frequently for IMDs for data transmission, remote monitoring, or wireless telemetry [7]. In Refs. [8, 9], the antenna was largely designed, and the SAR value was not measured, however [10], The SAR was measured, and it was equal to 0.145 W/KG for 10 g, in addition to the large size of the antenna, however the papers [11, 12]. It obtained a smaller antenna volume than previous research with SAR calculations equal to 0.134 and 0.160 W/kg for 10 g. The nano-antenna in healthcare offers high-resolution imaging, diagnostics, and non-invasive devices, enhancing directivity, signal clarity, and real-time monitoring for tissue characterization and monitoring [13]. Using MIMO diversity can improve data transmission for wearable devices in healthcare IoT applications [14]. Energy Efficiency for Low-Power Devices Enhanced LDPC performance can reduce retransmissions and processing overhead, leading to lower energy consumption. These implantable and wearable biomedical devices will be very useful, as energy efficiency is one of the most important foundations of medical antenna design [15]. The energy-saving methods described in this paper can be adapted to biocompatible devices. For example, low-power implantable sensors can benefit from optimal energy allocation to maintain information coherence without high power consumption [16]. Medically compatible devices used for social networking, such as micro-sensors and small internet data, can be combined with simple basic data and separate wavelet conversion to ensure secure data transmission over wireless communication systems, especially those supported by dedicated medical antennas [17]. Real-valued Fourier Transform algorithms can be used to process signals from biomedical devices in real time, aiding in applications like remote health monitoring, diagnostics, and emergency alerts [18]. This study presents a dual-band microstrip patch antenna for healthcare applications. By using a square spiral antenna design, one can miniaturize the size of an antenna to a suitable size. The antenna was implanted in voxel data/skin material in CST because the aim is to study the effect of implantation for medical purposes. Low SAR values and allowable input power have been calculated and negative gain for the three designs was achieved for safety considerations.

2.THEORETICAL

The resonance frequency is initially picked to design a microstrip antenna, followed by the selection of the antenna's dielectric constant. Eq. (1) expressed below can be used to calculate the width of the patch (W) [19]:

$$\boldsymbol{W} = \frac{C_0}{2f_r}\sqrt{\frac{2}{\epsilon_r+1}} \qquad (1)$$

Where W is the width of the patch antenna, f_r is the resonant frequency, C_0 is the light speed, and ϵ_r is the permittivity of the substrate.

The radiation propagating from the patch toward the ground passes through the air and sometimes through the dielectric (fringing). The effective refractive index value of a patch is a significant parameter that structures the patch antenna. Eq. (2) [19] was used to calculate the effective dielectric ($\epsilon_r ff$) value, taking into account the differences in permittivity between the air and the dielectric substrate.

$$\epsilon_r ff = \frac{\epsilon_r+1}{2} + \frac{\epsilon_r-1}{2}\left[\frac{1}{\sqrt{\frac{1}{1+12\frac{h}{\omega}}}}\right] \qquad (2)$$

Where h is substrate height.

Fringing causes an increase in antenna length (ΔL) electrically. The length ΔL of the antenna can calculated by Eq. (3) [20]:

$$\frac{\Delta L}{h} = 0.412 \frac{(\epsilon_r ff + 0.3)\left(\left(\frac{W}{h}\right) + 0.264\right)}{(\epsilon_r ff + 0.258)\left(\left(\frac{W}{h}\right) + 0.8\right)} \qquad (3)$$

Finally, the actual patch's length (L), could be determined by Eq. (4) [20]:

$$L = \frac{C_0}{2 f_r \sqrt{\epsilon_\varepsilon ff}} - 2\Delta L \qquad (4)$$

3. DESIGN ANTENNA

The design process begins with developing a microstrip dual-band antenna using the biocompatible material Rogers 3010 as a substrate, selected for its high relative permittivity ($\varepsilon_r = 11.2$, $\tan\delta = 0.0035$) with a thickness of 0.25 mm, which enables a compact and efficient antenna structure. The dimensions of the (27.6 mm × 28.2 mm × 0.32 mm), provide an optimized size suitable for dual-band performance as shown in Fig. 1. The substrate's properties and patch thickness are carefully considered to ensure appropriate impedance matching (50 Ω) and effective dual-frequency resonance. The radiating patch of the antenna is carefully sized and is characterized by a fractal structure for miniaturization because the antenna's physical length is reduced by meandering the antenna patch and also to get the target frequency bands, enabling dual-band operation for applications like medical applications, cellular, or Wi-Fi. An attractive choice for incorporation into modern communication systems, the RO3010's high dielectric constant improves the antenna's ability to produce stable dual-band performance within a small footprint.

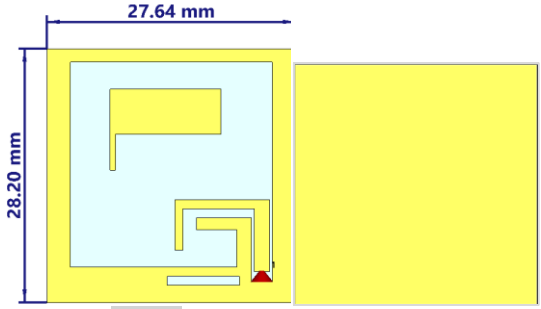

Fig. 1 Proposed Antenna.

The design steps for the final shape are explained as follows:

1- Choice of substrate and dimensions:
- A substrate measuring 27.64 mm × 28.20 mm was selected. These small dimensions were designed to meet the specifications of a compact antenna used in healthcare monitoring or medical applications.
- A medical-grade, biocompatible material, Rogers 3010, was used to ensure patient safety from wearable or implantable devices.

2- Patch design:
- The antenna's electrical length is increased due to the helical or folded patch design. This allows the antenna to resonate at specific ISM frequencies (0.9 GHz, 2.4 GHz, or 5.8 GHz) with these small dimensions.
- The electrical path was optimized without increasing the overall dimensions by using zigzag or fractal patterns.

3- Ground and feed design:
- The design incorporates a fully grounded design to ensure optimal impedance matching and electromagnetic isolation.
- The red triangle indicates the antenna feed point, where the coaxial feed line connects to the antenna. Impedance matching is a critical specification for the feed line, which must have a resistance of 50Ω.

4- Optimization Using Simulation Tools:
- The design was built and optimized using CST Studio Suite, which provides tools for simulating antenna performance (such as S11, gain, and radiation pattern). The results are very close to reality with a very small margin of error.
- The final antenna configuration, including substrate thickness, permittivity, and patch geometry, was achieved through trial and error.

The S-parameter plot in Fig. 2. shows the antenna's return loss. Values below -10 dB indicate good performance, meaning low reflection at 0.9 GHz and 2.45 GHz frequencies. These frequencies are fundamental and within the Intended Standard Modulation (ISM) range, indicating that the antenna radiates efficiently at these frequencies. Flatter areas represent poor synchronization and higher reflection near 0 dB. The narrow bandwidth of an antenna results from certain design methods and material choices, including a high-permittivity substrate, small antenna size, and a helical or zigzag structure. A full ground surface improves insulation but reduces the antenna's bandwidth, while precise impedance matching enhances performance at specific frequencies, further narrowing the operating frequency range. The narrow bandwidth characteristic of an antenna is a result of the trade-offs made to achieve small size, high efficiency, and precise frequency targeting. While narrow bandwidth antennas are well-suited for applications requiring precise frequency performance, such as biomedical applications, they will limit the antenna's ability to operate across wider frequency bands. [21].

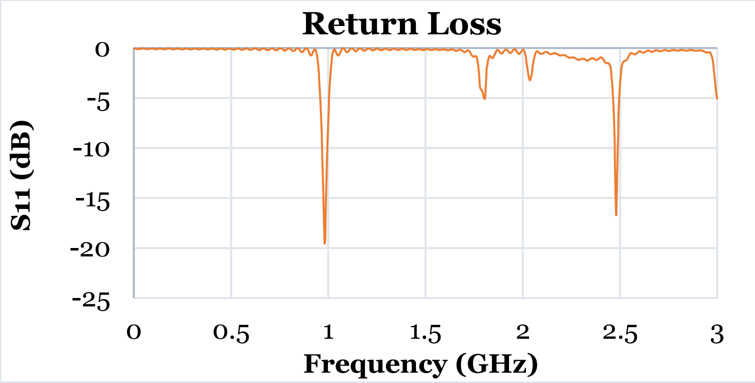

Fig. 2 S11 of the Proposed Antenna.

3.1. Implantable Antenna Design

The performance of the antenna is further examined by adding a 60 × 60 mm² layer of skin-mimicking material to the bottom layer as shown in Fig. 3. The skin layer is placed in contact with the antenna from below. The aim of this design is to evaluate the antenna's performance in terms of Specific Absorption Rate (SAR) and resonant frequency stability when placed on a material that mimics body tissue. This allows for the identification of resonant frequency variations and the measurement of SAR levels, ensuring compliance with global health and safety regulations by simulating the position of skin beneath the antenna. This additional layer helps in understanding the antenna's behavior under real-world operating conditions, providing valuable insights into its efficacy and safety in near-body medical applications.

component1:Skin	
Material	Voxel Data/Skin
Type	Normal
Epsilon	69.45
Electric cond.	0.507 [S/m]
Mu	1
Rho	1100 [kg/m^3]
Thermal cond.	0.3 [W/K/m]
Specific heat	3500 [J/K/kg]
Diffusivity	7.79221e-08 [m^2/s]
Bloodflow	9000 [W/K/m^3]
Metabolic rate	2000 [W/m^3]

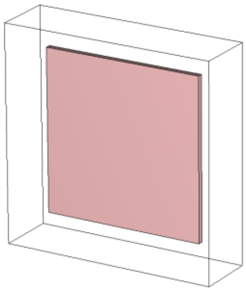

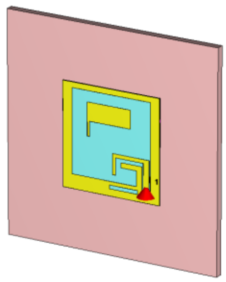

Fig. 3 Implantable Antenna and Skin Layer Performance.

The skin layer influences the antenna's impedance matching and resonant frequencies, in addition to the deeper and slightly shifted S11 dips as shown in Fig. 4. The strong insulation properties of the added layer increase the permittivity and electrical conductivity of the current, resulting in a lower S11 response frequency. This, in turn, increases resonance and energy absorption, thus reducing the antenna's resonant frequency. The designed dual-band microstrip antenna operates most accurately at two primary frequencies: 0.9 GHz and 2.4 GHz, both within the ISM band. Return loss (S11) values have been optimized at these frequencies to ensure accurate signal transmission and minimal reflection. The strong resonant S11 value at 0.9 GHz enables efficient performance in the lower bands. The second effective frequency for the medical antenna, 2.4 GHz, is used in higher-frequency applications. One of the most important specific applications for this type of antenna is continuous glucose monitoring for patients with chronic diabetes, where the antenna transmits data from a sensor implanted inside the patient's body to an external receiver for continuous glucose monitoring.

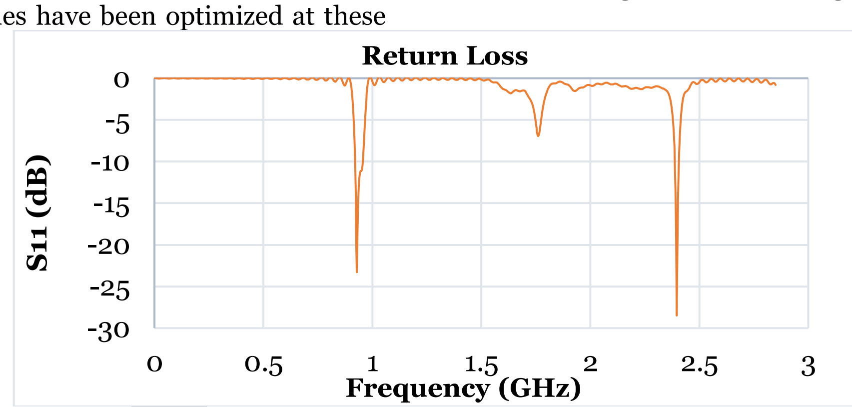

Fig. 4 S11 of Implantable Antenna with Skin Layer.

Figure 5 shows the antenna's far-field pattern and gain. The gain of the presented antenna at the E plane is -29.4 and -13 dBi at 0.9 GHz and 2.45 GHz respectively, which is considered safety for medical purposes. The electrical size of the antenna at various frequencies causes variations in radiation patterns that impact current distribution. Higher-order modes and edge effects produce a directional pattern at 0.9 GHz, whereas the antenna supports the fundamental mode at 2.45 GHz, resulting in an omnidirectional pattern. Ground plane interactions further influence the radiation.

3.2. Wearable Antenna Design

In this step, the antenna is modified into an arc shape to leverage the flexibility of the Rogers RO3010 material as shown in Fig. 6. The aim is to study its performance when worn on the wrist, as in a smartwatch application. By curving the antenna to mimic the natural contour of the human wrist, a realistic usage scenario for wearable medical technology is simulated.

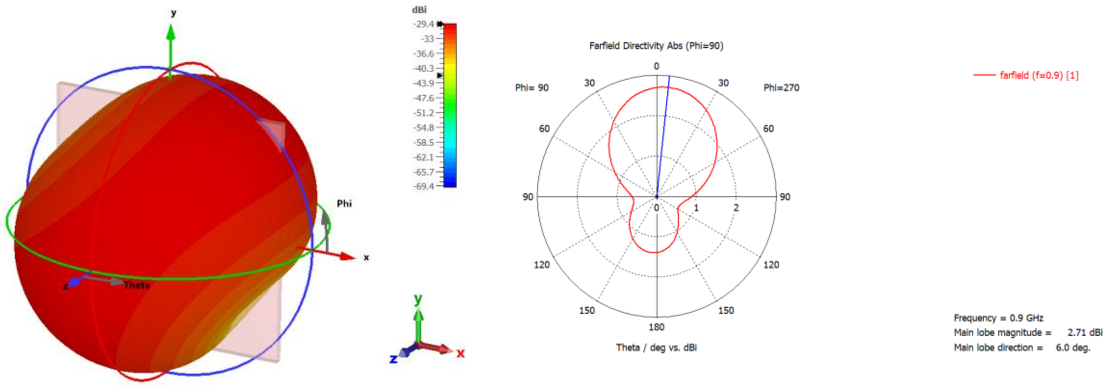

(a)

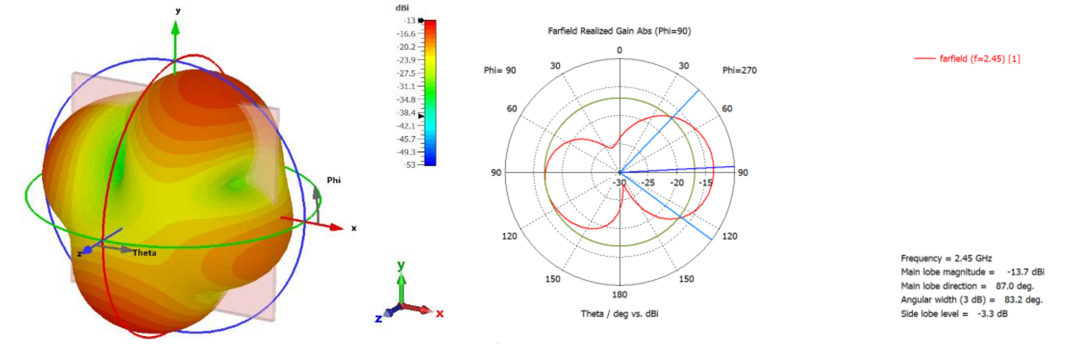

(b)

Fig. 5 1D and 3D Pattern (a) at 0.9 GHz, and (b) at 2.4 GHz.

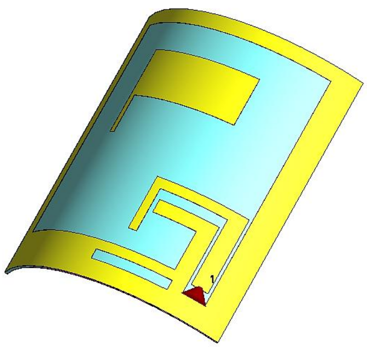

Fig. 6 Wearable Antenna.

The arc-shaped modification of the antenna introduced additional operating bands, plot Fig. 7., high S11 resonances appear at 0.9 GHz and 2.4 GHz (ISM band), while low S11 values at 0.98 GHz and 2.9 GHz indicate unwanted frequencies. The S-parameter plot confirms a significant S11 reduction at the target frequencies of 0.9 GHz and 2.4 GHz. To assess the arc-shaped antenna's effectiveness close to human tissue, a skin-equivalent material layer was put underneath it to replicate a realistic usage scenario Fig. 8. To investigate the human body's maximal impact, the skin layer was planted in close touch with the antenna. The presence of the skin layer provides insights into potential shifts in resonant frequencies and signal behavior due to tissue interaction.

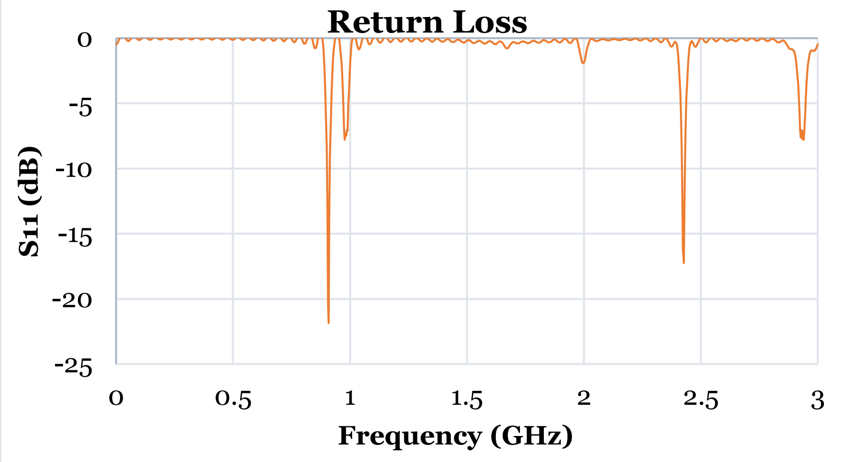

Fig. 7 S11 of Wearable Antenna.

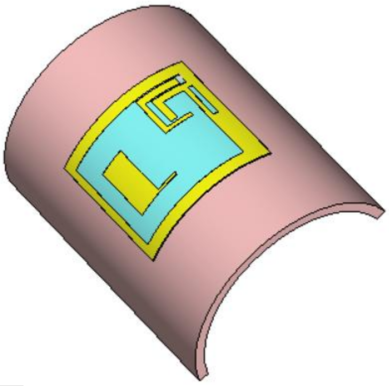

Fig. 8 Wearable Antenna with Skin Layer.

Including the skin layer in Fig. 9 marginally expands the bandwidth compared to Fig. 7. This is indicated by a slightly wider bandwidth, suggesting that the antenna with the skin layer helped in improving the matching over a wider band. With the addition of the skin-equivalent material beneath the arc-shaped antenna, a downward shift in the resonant frequencies was observed. S11 was at the range, peaking at the 2.4 GHz band and 915 MHz (ISM), as shown in Fig. 10.

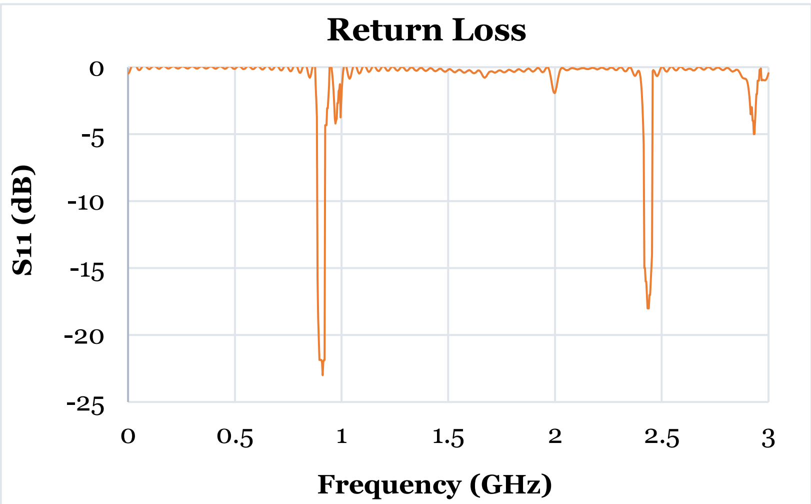

Fig. 9 S11 of Wearable Antenna with Skin Layer.

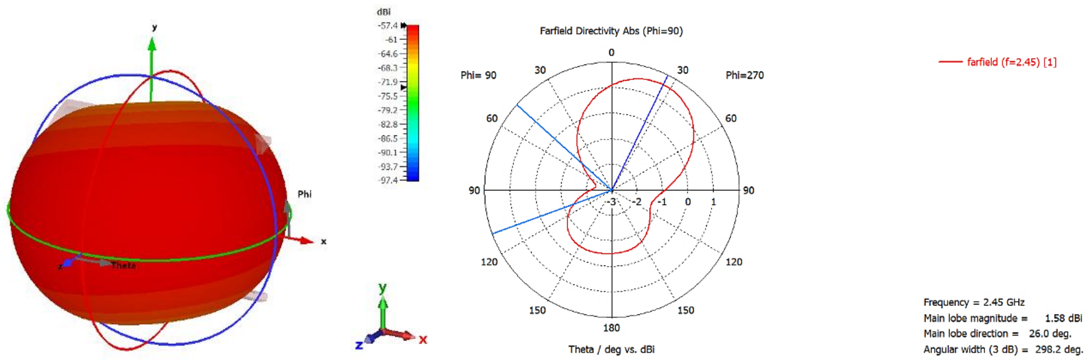

(a)

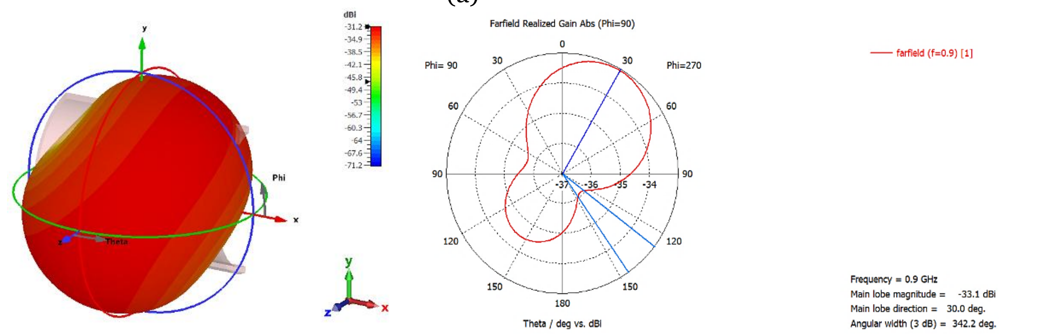

(b)

Fig. 10 1D and 3D Pattern of Wearable with Skin (a) 2.4 GHz (b) 0.9 GHz.

Differences in radiation patterns at different frequencies owing to antenna electrical size affect current distribution. Negative gain in medical antennas is an important factor for patient safety.

3.3.Capsule Antenna Design

The antenna is reconfigured into a capsule shape to further increase its adaptability and compactness, greatly lowering its overall size without sacrificing functionality, as shown in Fig. 11. The antenna's physical factor makes it appropriate for a range of uses outside of wearable technology, such as incorporation into small devices like tracking systems, medical implants, and sensors for health monitoring. The capsule antenna shown is typically used for wireless capsule endoscopy. In this medical application, the antenna enables real-time communication between a swallowed capsule (equipped with a camera or sensors) and an external receiver. This allows gastrointestinal tract monitoring to diagnose issues like ulcers, bleeding, or tumors. Figure 12 shows the capsule-shaped antenna's resonance frequencies at 0.9 GHz (single-band ISM), which demonstrates its capacity to function efficiently throughout these important communication bands. The 2.4 GHz resonance vanished due to the antenna's curvature, which altered the effective electrical length and impedance matching. This structural change impacted resonance conditions, shifting or suppressing the expected frequency response.

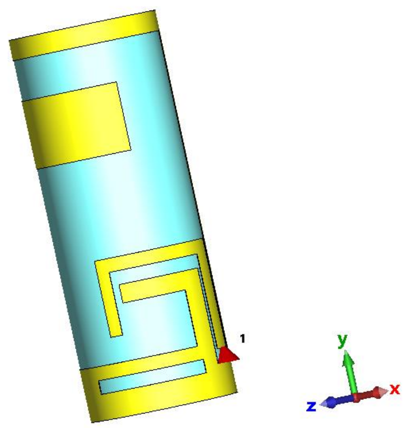

Fig. 11 Capsule Antenna.

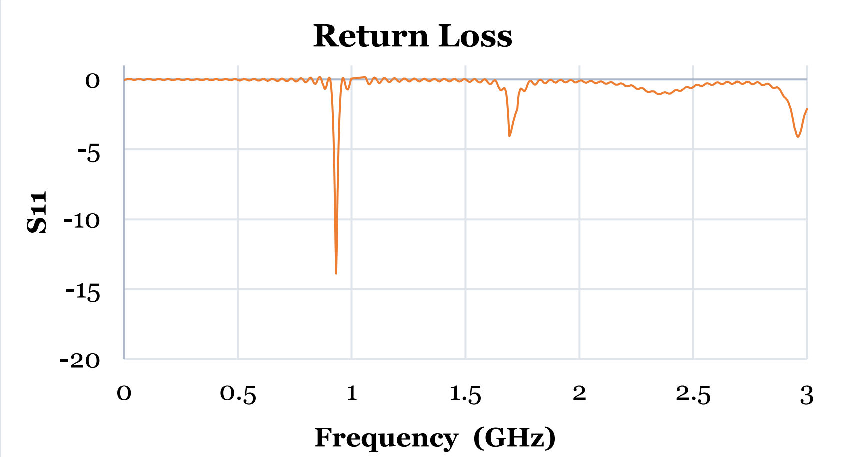

Fig. 12 S11 of Capsule Antenna.

Figures 13 show the gain equal to -43.6 dBi and far-field pattern.

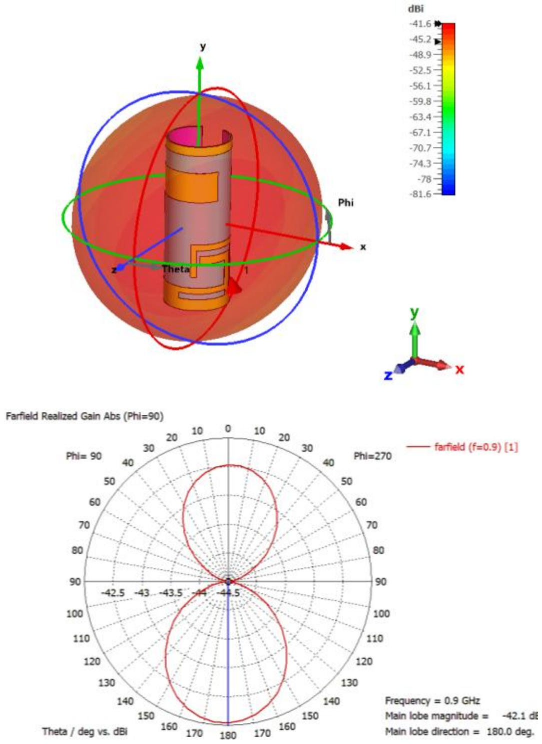

Fig. 13 1D and 3D Pattern of Capsule Antenna at 0.9 GHz.

4.SAR CALCULATION AT HUMAN BODY

"The IEEE C95.1-1999 standard restricts the SAR averaged over 1 g of tissue to less than 1.6 W/Kg" [22]. While the input power across 1 g volume tissue can vary based on the specific design and operational frequency of the antenna, it is generally kept low (often under 10 mW) to maintain SAR levels within safe limits as defined by regulatory standards. In this study, 1 mW was used to get an acceptable value of SAR.

4.1.SAR of Implantable

The proposed simulation results revealed a SAR value of 0.487 and 0.141 W/kg at the operational frequencies 0.9 and 2.4 GHz respectively in Fig. 14, which falls well within the recommended safety limits set by regulatory bodies.

4.2.SAR of Wearable

The simulation results indicated a SAR value of 0.0488 W/kg at 0.9 GHz and 0.0392 W/kg at 2.4 GHz, as shown in Fig. 15, within the safety limitations established by regulatory authorities.

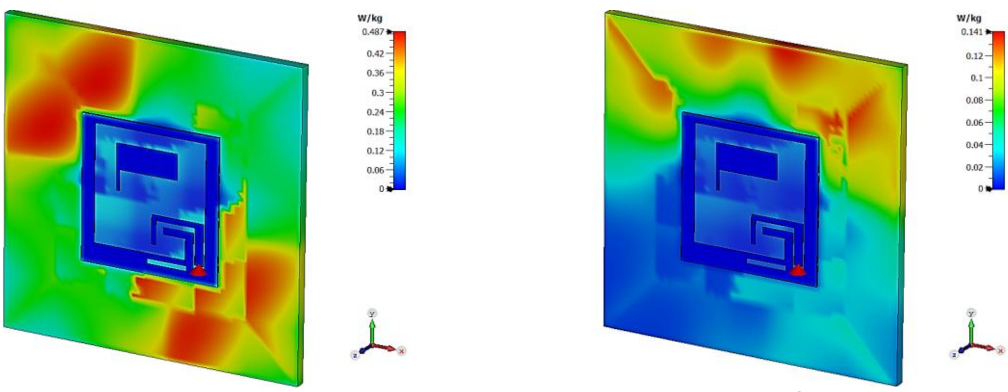

(a) (b)

Fig. 14 SAR Simulation of Implantable Antenna (a) 0.9 GHz (b) 2.4 GHz.

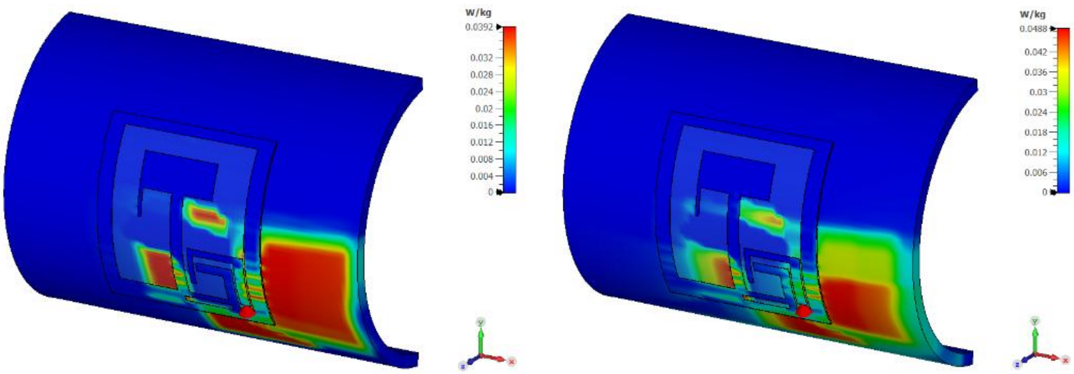

Fig. 15 SAR Simulation of Wearable Antenna (a) 0.9 GHz (b) 2.4 GHz.

5.COMPARISON PROPOSED ANTENNA WITH OTHER

From Table 1, this work presents a compact antenna operating at 0.9 GHz, and 2.45 GHz with miniaturized size, making it smaller than many others listed and ideal for wearable or implantable applications. Its frequency range covers common bands used in medical and communication (e.g., 2.45 GHz for heart rate, oxygen levels, and blood pressure). Table 1 illustrates the trend towards smaller, multi-band antennas that ensure safety (low SAR) for medical and wearable use. Overall, it showcases advances in antenna design emphasizing miniaturization, multi-band support, and safety adherence.

Table 1 Proposed Antenna Comparison with Another Research.

Ref.	Frequency	Size (mm)	SAR
[8]	2.4, 3.4 GHz	70 × 70	N/A
[9]	1 GHz, 2.4 GHz	60 × 60	N/A
[10]	4.27 GHz, 5.8 GHz,	62 × 58	0.145 W/kg for 10 g
[11]	2.45 GHz, 4.27 GHz	50 × 50	N/A
[23]	1.6 GHz, 2.4 GHz	40 × 40	N/A
[12]	1.575 GHz, 2.4 GHz	85.5 × 85.5	0.134 and 0.160 W/kg for 10 g
[24]	2.4 GHz, 5.8GHz	52.3 × 58.69	0.326 and 1.024 W/kg for 1g
[25]	2.45 GHz	43 × 30	N/A
This work	0.9 GHz, 2.4 GHz	27.6 × 28.2	0.478, 0.141, 0.0488, and 0.0392 for 1g

6.CONCLUSIONS

In this paper, a miniature microstrip dual-band antenna with a size (of 27.6 mm × 28.2 mm × 0.32 mm) was developed for biomedical applications with low SAR levels for implantable and wearable designs which is equal to (0.487, and 0.141 W/kg) and (0.488, and 0.0392 W/kg) for dual bands 0.9 and 2.4 GHz respectively. Several ISM bands in this antenna were achieved by developing and designing the antenna's structure. Simulation outcomes showed very good agreement as to the performance of the presented implantable antenna despite the miniaturized size and in comparison, with prior implantable dual-band printed antennas.

CREDIT AUTHORSHIP CONTRIBUTION STATEMENT

Abu Obaydah N. Khazaal: Writing – original draft, review, Visualization, Validation, Methodology, Designing, Investigation, Formal analysis, Data curation, Funding acquisition. *Mohammad K. S. AL-Mashhadani*: Editing, Supervision, Resources, Project administration, Methodology, Conceptualization.

DECLARATION OF COMPETING INTEREST

The authors declare that they have no known competing financial interests or personal relationships that could have appeared to influence the work reported in this paper.

ACKNOWLEDGEMENTS

The authors are grateful for the financial support for this research from the Electrical Engineering Department, College of Engineering, Tikrit University. Postgraduate Research Grant (PGRG) No.TU.G/2022/HIR/MOHE/ENG/623 (24470-7-3).

REFERENCES

[1] Hu X-Y, Yin W-L, Du F, Zhang C, Xiao P, Li G. **Biomedical Applications and Challenges of In-Body Implantable Antenna for Implantable Medical Devices: A Review.** *AEU - International Journal of Electronics and Communications* 2024; **174**: 155053.

[2] Hu X-Y, Liu Z, Li G. **Implantable Devices Based on Ultra-Wideband Miniaturized Implantable Antenna for Biotelemetry Application.** *2023 International Applied Computational Electromagnetics Society Symposium (ACES-China)* 2023; Hangzhou, China. IEEE: p. 1-3.

[3] Chishti AR, Aziz A, Aljaloud K, Tahir FA, Abbasi QH, Khan ZU, Hussain R. **A Sub 1 GHz Ultra Miniaturized Folded Dipole Patch Antenna for

Biomedical Applications. *Scientific Reports* 2023; **13**: 9900.

[4] Bahrouni M, Houzet G, Vuong TP, Mendes PM, Dinis H, Silva R, Trabelsi H. **Modeling of a Compact, Implantable, Dual-Band Antenna for Biomedical Applications.** *Electronics* 2023; **12**(6): 1475.

[5] Samy MRKM, Gudipalli A. **A Review on Miniature Bio-Implant Antenna Performance Enhancement and Impact Analysis on Body Fluids in Medical Application.** *Measurement: Sensors* 2023; **28**: 100849.

[6] Dash S, Mohanty SK. **Selection of Suitable Dielectric Substrate for Miniaturization of Microstrip Patch Antenna Using DGS Fractals.** *Recent Advances in Electrical & Electronic Engineering* 2022; **15**(8): 688-697.

[7] CFR. **Federal Communications Commission: Industrial, Scientific, and Medical Equipment.** *Telecommunication. Code of Federal Regulations*; 1985.

[8] Yang H, Liu X. **Wearable Dual-Band and Dual-Polarized Textile Antenna for On- and Off-Body Communications.** *IEEE Antennas and Wireless Propagation Letters* 2020; **19**(12): 2324-2328.

[9] Khajeh-Khalili F, Haghshenas F, Shahriari A. **Wearable Dual-Band Antenna with Harmonic Suppression for Application in Medical Communication Systems.** *AEU - International Journal of Electronics and Communications* 2020; **126**: 153396.

[10] Kumar D, Mathur D. **Novel Design of a Bandwidth Enhanced and Frequency Reconfigurable, Wearable Antenna for Body Centric Communication.** *Journal of Electromagnetic Engineering and Science* 2024; **24**(3): 264-275.

[11] Sung Y. **Wideband Circularly Polarized Antenna for Dual-Band Operation.** *Microwave and Optical Technology Letters* 2021; **63**(1): 286-294.

[12] Joshi R, Hussin EFNM, Soh PJ, Jamlos MF, Lago H, Al-Hadi AA, Podilchak SK. **Dual-Band, Dual-Sense Textile Antenna with AMC Backing for Localization Using GPS and WBAN/WLAN.** *IEEE Access* 2020; **8**: 89468-89478.

[13] Saleem AE, Hasan JA. **Metamaterial-Based Nano-Antenna Design of Enhanced Plasmonic Electromagnetic Properties.** *Tikrit Journal of Engineering Sciences* 2024; **31**(3): 266-274.

[14] Abdulsada SS, Hassib MD, Jameel ZN. **Underwater Wireless Optical Communication for IOT Using Coding MIMO Diversity.** *Tikrit Journal of Engineering Sciences* 2024; **31**(1): 152-160.

[15] Al-Kadhimi AM, Abdulkareem AE, Tsimenidis CC. **Performance Enhancement of LDPC Codes Based on Protograph Construction in 5G-NR Standard.** *Tikrit Journal of Engineering Sciences* 2023; **30**(4): 1-10.

[16] Saeed SH, Sileh IK. **Performance Analysis of Cooperative NOMA for Different Power Allocation Strategies.** *Tikrit Journal of Engineering Sciences* 2023; **30**(4): 102-117.

[17] Abdullah SF, Nawaf SF. **Optimizing Data Security with Hybrid Scheme Based on LSB and DWT.** *Tikrit Journal of Engineering Sciences* 2023; **30**(3): 190-199.

[18] Salih SK, Hamood MT. **New Algorithm for Real-Valued Fourier Transform.** *Tikrit Journal of Engineering Sciences* 2023; **30**(4): 127-133.

[19] Balanis CA. **Antenna Theory: Analysis and Design.** *John Wiley & Sons*; 2015.

[20] Garg R. **Microstrip Antenna Design Handbook.** *Artech House*; 2001.

[21] Arnaoutoglou DG, Empliouk TM, Kaifas TN, Chryssomallis MT, Kyriacou G. **A Review of Multifunctional Antenna Designs for Internet of Things.** *Electronics* 2024; **13**(16): 3200.

[22] Abdul-Al M, Amar A, Tamer I, Littlehales R, Ojaroudi Parchin N, Al-Yasir Y, See CH, Zhou D, Zainal Abidin Z, Alibakhshikenari M, Zebiri C, Elmegri F, Abusitta MM, Ullah A, Fathi M, Abdussalam A, Rodriguez J, McEwan NJ, Noras JM, Abd-Alhameed R. **Wireless Electromagnetic Radiation Assessment Based on the Specific Absorption Rate (SAR): A Review Case Study.** *Electronics* 2022; **11**: 511.

[23] George U, Lili F. **A Simple Frequency and Polarization Reconfigurable Antenna.** *Electromagnetics* 2020; **40**(6): 435-444.

[24] Rachman FA, Rahardjo ET. **Design of a Dual-Band Wearable Antenna Operating at 2.45 GHz and 5.8 GHz for Medical Communication Applications.** *International Journal of Electrical, Computer, and Biomedical Engineering* 2024; **2**(1): 101-114.

[25] Ali SH, Alfalahi AH, Hachim YA. **A Miniaturized Compact Wideband Partial Ground Antenna Used in RFID Systems.** *Tikrit Journal of Engineering Sciences* 2020; **27**(2): 40-45.